

Enhancement by Uridine Diphosphate of Macrophage Inflammatory Protein-1 Alpha Production in Microglia Derived from Sandhoff Disease Model Mice

Eri Kawashita · Daisuke Tsuji · Yosuke Kanno ·
Kaho Tsuchida · Kohji Itoh

Received: 09 June 2015 / Revised: 26 August 2015 / Accepted: 08 September 2015 / Published online: 7 November 2015
© SSIEM and Springer-Verlag Berlin Heidelberg 2015

Abstract Sandhoff disease (SD) is a lysosomal β -hexosaminidase (Hex) deficiency involving excessive accumulation of undegraded substrates, including GM2 ganglioside, and progressive neurodegeneration. Macrophage inflammatory protein-1 α (MIP-1 α) is a crucial factor for microglia-mediated neuroinflammation in the onset or progression of SD. However, the transmitter-mediated production of MIP-1 α in SD is still poorly understood.

Extracellular nucleotides, including uridine diphosphate (UDP), leaked by either injured or damaged neuronal cells activate microglia to trigger chemotaxis, phagocytosis, macropinocytosis, and cytokine production.

In this study, we demonstrated that UDP enhanced the production of MIP-1 α by microglia derived from SD mice (SD-Mg), but not that from wild-type mice (WT-Mg). The UDP-induced MIP-1 α production was mediated by the activation of P2Y6 receptor, ERK, and JNK. We also found the amount of dimeric P2Y6 receptor protein to have

increased in SD-Mg in comparison to WT-Mg. In addition, we demonstrated that the disruption of lipid rafts enhanced the effect of UDP on MIP-1 α production and the disordered maintenance of the lipid rafts in SD-Mg. Thus, the accumulation of undegraded substrates might cause the enhanced effect of UDP in SD-Mg through the increased expression of the dimeric P2Y6 receptors and the disordered maintenance of the lipid rafts. These findings provide new insights into the pathogenic mechanism and therapeutic strategies for SD.

Introduction

Sandhoff disease (SD) is a progressive neurodegenerative disorder caused by a defect of the β -hexosaminidase (Hex) β -subunit gene, which is associated with deficiencies of HexA ($\alpha\beta$) and HexB ($\beta\beta$) (Mahuran 1999). In SD, an excessive accumulation of undegraded substrates, including GM2 ganglioside, is observed, particularly within lysosomes in the neuronal cells, due to the deficiencies of HexA and HexB. These deficiencies lead to neurological symptoms in the central nervous system (CNS), such as mental retardation, spasms, and quadriplegia. Several therapeutic approaches for SD have been investigated for decades, including substrate reduction therapy (Wortmann et al. 2009), bone marrow transplantation (Norflus et al. 1998; Wada et al. 2000), stem cell therapy (Lee et al. 2007), enzyme replacement therapy (Matsuoka et al. 2010), and gene therapy (Bradbury et al. 2013), where the aim is to reduce the accumulated substrates. Although the cause of SD is obvious, the disease remains incurable thus far.

SD model mice (SD mice), established by means of Hex β -subunit gene disruption, exhibit neurological manifestations quite similar to those observed in SD patients (Sango

Communicated by: Johannes Häberle

Competing interests: None declared

Electronic supplementary material: The online version of this chapter (doi:10.1007/8904_2015_496) contains supplementary material, which is available to authorized users.

E. Kawashita
Department of Pathological Biochemistry, Kyoto Pharmaceutical University, Yamashina-ku, Kyoto, Japan

Y. Kanno · K. Tsuchida
Department of Clinical Pathological Biochemistry, Faculty of Pharmaceutical Science, Doshisha Women's College of Liberal Arts, Kyotanabe, Kyoto, Japan

D. Tsuji · K. Itoh (✉)
Department of Medicinal Biotechnology, Institute for Medicinal Research, Graduate School of Pharmaceutical Sciences, Tokushima University, 1-78 Sho-machi, Tokushima 770-8505, Japan
e-mail: kitoh@tokushima-u.ac.jp

et al. 1995). Previous studies revealed the progressive increase in microglial activation/expansion and the following neuronal apoptosis in the brain of SD mice, suggesting that microglial inflammation is most likely involved in the neurodegenerative mechanism in SD (Wada et al. 2000; Jeyakumar et al. 2003). Our previous studies demonstrated that macrophage inflammatory protein-1 α (MIP-1 α) is upregulated in the brains of SD mice during the pathogenesis and in microglial cells derived from SD mice (Tsuji et al. 2005; Kawashita et al. 2009). Wu and Proia also demonstrated that MIP-1 α is responsible for the recruitment of macrophages/microglia from the periphery in the pathogenic process of SD, and the deletion of the MIP-1 α gene increases the life span of SD mice (Wu and Proia 2004). These studies suggest that MIP-1 α is a crucial factor for microglia-mediated neuroinflammation in SD, and the downregulation of the abnormal production of MIP-1 α by microglia could therefore delay the onset or progression of SD.

Microglia monitor the environment in the CNS under normal conditions; however, they become activated when they recognize a pathological state in the brain (Nimmerjahn et al. 2005). Injured or damaged neuronal cells activate microglia through the leakage of extracellular nucleotides, adenosine triphosphate and uridine diphosphate (ATP and UDP, respectively), to trigger chemotaxis, phagocytosis, macropinocytosis, and cytokine production (Davalos et al. 2005; Koizumi et al. 2007; Kim et al. 2011; Uesugi et al. 2012; Ikeda et al. 2013). The extracellular nucleotides modulate cellular function by activating purinergic (P2) receptors, which are classified into ionotropic P2X receptors and metabotropic P2Y receptors. Microglia have been shown to express functional P2X4, P2X7, P2Y6, and P2Y12 receptors. These studies suggest that extracellular nucleotide signaling should engage in a pathological event in the brain.

The present study aimed to investigate the effect of extracellular nucleotides on the production of MIP-1 α by microglia derived from SD mice and wild-type mice (SD-Mg and WT-Mg, respectively) and elucidate the underlying mechanisms.

Materials and Methods

Cell Culture

Microglia were prepared from the cerebra of 1-day-old SD (*Hexb*^{-/-}) (Sango et al. 1995) and WT (*Hexb*^{+/+}) mice as described in previous study (Kawashita et al. 2009). The cells were maintained in Dulbecco's Modified Eagle's Medium (DMEM), supplemented with 10% fetal bovine serum (FBS), 5 μ g/mL insulin, 1 μ g/mL granulocyte-

macrophage colony-stimulating factor (GM-CSF), 0.1 mg/mL streptomycin, and 100 U/mL penicillin G, at 37°C in an incubator in the presence of 5% CO₂.

Enzyme-Linked Immunosorbent Assay for MIP-1 α Production

The cells plated on 96-well plates (2×10^4 cells/well) were treated with UDP or ATP for 6 h. For inhibition assay, the cells were pretreated for 30 min with Reactive Blue 2, suramin, MRS2578, MK571, PD98059, and SP600125 before stimulated with UDP. The conditioned medium (CM) was centrifuged at $2,300 \times g$ for 5 min. The MIP-1 α levels in the resultant supernatants were measured with a mouse MIP-1 α immunoassay kit (Quantikine M, R&D Systems, Minneapolis, MN, USA).

Reverse Transcription-Polymerase Chain Reaction (RT-PCR) Analysis

Total RNA was isolated from the cells using TRIsure (Bioline, London, UK). After addition of CHCl₃, centrifugation was performed at $15,000 \times g$ for 15 min. The resultant supernatants were each mixed with an equal volume of 2-propanol. After centrifugation, the pellets were rinsed with 75% ethanol/diethylpyrocarbonate (DEPC)-treated water and then dried. The pellets were each dissolved in an appropriate volume of DEPC-treated water as total RNA fractions. RNA from each sample (1 μ g) was transcribed using ReverTra Ace- α (Toyobo, Osaka, Japan) according to the manufacturer's protocol. In PCR assay, murine P2Y6 receptor and glyceraldehyde 3-phosphate dehydrogenase (GAPDH) mRNA were amplified in reaction mixtures consisting of GoTaq reaction buffer (Promega, Madison, WI, USA), dNTPs, GoTaq DNA polymerase, cDNA solution, and each primer. An equal amount of amplified products was subjected to electrophoresis, stained with ethidium bromide, and then visualized under UV light. Quantitative PCR for murine P2Y6 mRNA expression relative to GAPDH mRNA expression was performed using a MiniOpticon real-time PCR system according to the manufacturer's protocol (Bio-Rad Laboratories, Hercules, CA, USA). The primer sequences for P2Y6 were 5'-GGAACACCAAATCTGGCACTTCC-3' (sense) and 5'-GTATACCGGGTTAGCAGCAGTC-3' (antisense), and the sequences for GAPDH were 5'-TTCATTGACCTCAACTACATG-3' (sense) and 5'-GTGGCAGTGATGCATGGAC-3' (antisense).

Immunoblotting

The cells were washed twice with cold PBS, harvested, and then sonicated in 10 mM Tris-HCl buffer (pH 7.5)

containing 1% SDS, 1% Triton X-100, and a protease inhibitor cocktail (Roche, Mannheim, Germany). The protein concentration in each lysate was measured using a BCA protein assay kit (Pierce, Rockford, IL, USA). Lysates containing equal amounts of protein were subjected to SDS-polyacrylamide gel electrophoresis on a 10% acrylamide gel. Proteins were visualized by immunostaining with primary antibodies, secondary antibodies, and a chemiluminescence reagent (PerkinElmer Life Sciences, Boston, MA, USA). The primary antibodies were anti-P2Y6 rabbit antibody (1:1,000 dilution) (Abcam, Cambridge, UK), anti-GAPDH rabbit antibody (1:5,000 dilution) (Sigma), and anti-flotillin-1 goat antibody (1:1,000 dilution) (Santa Cruz Biotechnology, Inc., Santa Cruz, CA, USA). The secondary antibodies were HRP-labeled anti-rabbit IgG antibody (1:4,000 dilution) (GE Healthcare Bio-Sciences, Little Chalfont, UK) and HRP-labeled anti-goat IgG antibody (1:2,000 dilution) (Dako, Cambridge, UK). Densitometry analysis was performed using a RAS3000 image system (Fuji Film, Tokyo, Japan).

Immunocytochemistry

The cells were fixed with cold 4% *p*-formaldehyde (PFA) in PBS, washed with PBS, treated with 25 mM glycine in PBS for 30 min, and washed with PBS. The cells were treated with 0.5% Triton X-100 in PBS for 10 min, washed with PBS, and then immunostained by a two-step incubation method. In brief, the fixed cells were treated with antibodies against flotillin-1 (1:200 dilution) (Santa Cruz Biotechnology, Inc.) and GM2 (1:50 dilution) (Kotani et al. 1992) at 4°C overnight. After washing with PBS, they were treated with Alexa 488-labeled anti-goat IgG and Cy3-labeled anti-mouse IgG (1:400 dilution) (Jackson ImmunoResearch Laboratories, PA, USA), at room temperature for 2 h. The specimens were washed with PBS containing 0.05% Tween 20 and observed under a confocal fluorescent microscope (LSM510, Zeiss, Oberkochen, Germany). Fluorescence was excited by the 488-nm line of an argon laser and the 543-nm line of a helium/neon laser. Optical setting, including pinhole diameter and amplifier gain/offset, was constant in each experiment.

Results

UDP Induces MIP-1 α Production in SD-Mg but Not in WT-Mg

We first analyzed the effect of UDP or ATP on the production of MIP-1 α by WT- and SD-Mg. The baseline production of MIP-1 α was higher in SD-Mg than that in WT-Mg without treatment (Fig. 1a), which is in agreement

with our previous study (Kawashita et al. 2009). The amount of MIP-1 α in CM of SD-Mg increased after treatment with UDP compared with untreated SD-Mg, while there was little effect on the production of MIP-1 α by WT-Mg. In contrast, ATP had no effect on the production of MIP-1 α by WT- or SD-Mg (Fig. 1a). Additionally, the amount of MIP-1 α in the CM of SD-Mg after treatment with UDP exhibited a time-dependent increase (Fig. 1b). We also confirmed that UDP enhanced the production of MIP-1 α by SD-Mg at the transcriptional level (Supplementary Fig. 1).

P2Y6 Receptor and Activation of ERK and JNK Mediate UDP-Induced MIP-1 α Production in SD-Mg

UDP is a known ligand of the P2Y2 and P2Y6 receptors, in addition to the CysLT1 and CysLT2 receptors which are receptors for cysteinyl leukotrienes, while UTP that is converted from UDP by ecto-nucleoside diphosphokinase binds to P2Y2, P2Y4, and P2Y6 (von Kugelgen 2006). To determine the receptor involved in the UDP-induced MIP-1 α production in SD-Mg, we analyzed the effects of antagonists with affinity at P2Y receptors on UDP-induced MIP-1 α production in SD-Mg. Reactive Blue 2 is a well-known, highly potent P2Y receptor antagonist, and suramin is an effective broad-spectrum antagonist of P2Y receptors with the exception of the P2Y4 receptor (von Kugelgen 2006). Both Reactive Blue 2 and suramin markedly abolished UDP-induced MIP-1 α production in SD-Mg (Fig. 2a). We next analyzed the effect of the P2Y6-specific antagonist, MRS2578, on UDP-induced MIP-1 α production in SD-Mg. MRS2578 significantly reduced UDP-induced MIP-1 α production in SD-Mg in a dose-dependent manner (Fig. 2b). We also confirmed that the CysLT1-specific antagonist, MK571, had no effect on UDP-induced MIP-1 α production in SD-Mg (Fig. 2c), and UTP increased the amount of MIP-1 α in the CM of SD-Mg (Supplementary Fig. 2). The P2Y2 and P2Y4 receptors can be equally activated by UTP and ATP (von Kugelgen 2006). The CysLT1 and CysLT2 receptors do not respond to treatment with UTP or ATP, even when the triphosphate nucleotides are added at high micromolar concentrations (Mellor et al. 2001, 2003). As shown in Fig. 1a, ATP had no effect on the production of MIP-1 α by SD-Mg. Thus, these data demonstrated that UDP, and potentially UTP converted from UDP, induces the production of MIP-1 α by SD-Mg via the P2Y6 receptor, but not via the P2Y2 nor P2Y4 receptor.

Our previous study reported that the activation of ERK and JNK is involved in the abnormal production of MIP-1 α by SD-Mg (Kawashita et al. 2009, 2011). We examined whether the activation of ERK and JNK is also involved in UDP-induced MIP-1 α production in SD-Mg. An ERK inhibitor

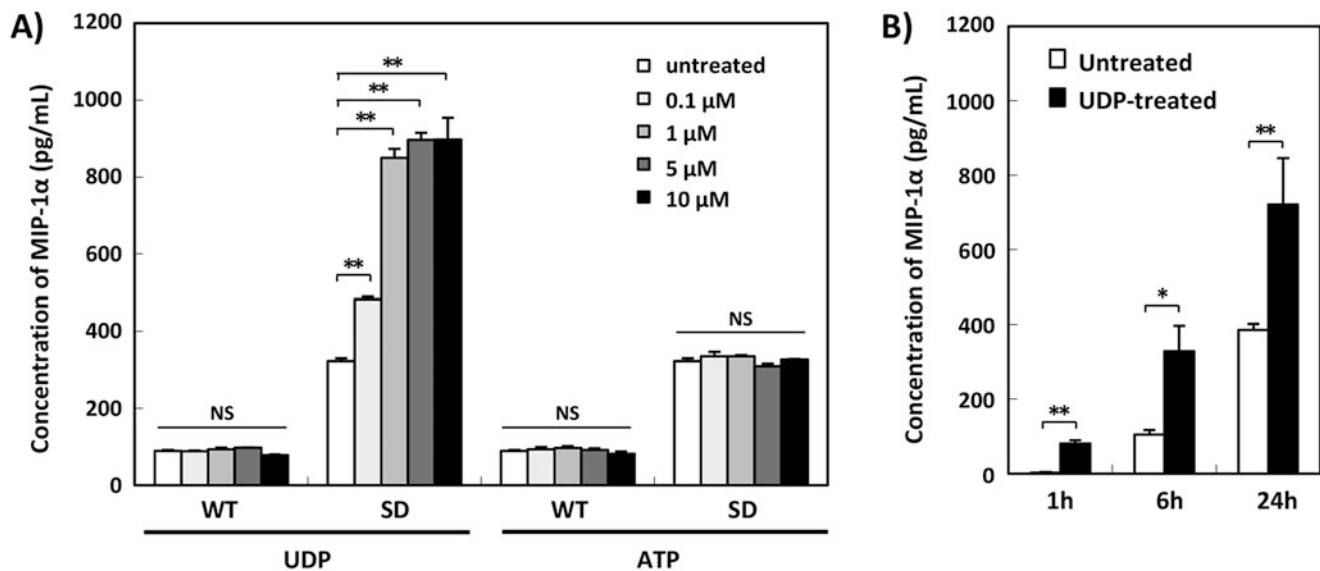


Fig. 1 Induction of MIP-1 α production by UDP in SD-Mg but not WT-Mg. (a) WT- and SD-Mg were treated with the indicated concentrations of UDP for 24 h, and then the amounts of MIP-1 α in the CM of the cells were measured using an ELISA kit ($n = 3$). (b)

SD-Mg were treated with UDP (5 μ M) for 1, 6, or 24 h ($n = 3$). Values represent the mean \pm S.E. Significance was evaluated using ANOVA with LSD post hoc test. * $P < 0.05$, ** $P < 0.01$

and JNK inhibitor, PD98059 and SP600125, respectively, inhibited the UDP-induced MIP-1 α production in SD-Mg in a dose-dependent manner (Fig. 2d, e), indicating that the activation of ERK and JNK mediates enhanced MIP-1 α production by treatment with UDP in SD-Mg.

Expression of the P2Y6 Receptor Is Increased in SD-Mg Compared with WT-Mg

We next analyzed the expression of the P2Y6 receptor in WT- and SD-Mg. The expression of the P2Y6 receptor was found to prominently increase in SD-Mg compared with WT-Mg at the transcriptional level (Fig. 3a). A real-time PCR analysis showed that the gene expression ratio of the P2Y6 receptor relative to GAPDH significantly increased in SD-Mg in comparison to WT-Mg (Fig. 3b). Furthermore, we analyzed the protein expression of the P2Y6 receptor in WT- and SD-Mg by immunoblotting using an antibody against the P2Y6 receptor. A recent study reported that P2Y6 receptors should be present in neuronal cells as monomeric and dimeric forms (D'Ambrosi et al. 2007). In this study, the endogenous P2Y6 receptor appeared as a 70 kDa protein band under a nonreducing condition, while the P2Y6 receptor appeared as 70 and 36 kDa protein bands under reducing conditions, with the molecular masses corresponding to both the monomeric and dimeric forms (Fig. 3c). The expression of P2Y6 receptors in dimeric forms significantly increased in SD-Mg compared with WT-Mg under both nonreducing and reducing conditions (Fig. 3d).

Disruption of Lipid Rafts Enhanced UDP-Induced MIP-1 α Production in WT- and SD-Mg

A recent study demonstrated that the monomeric P2Y6 receptor protein displays a selective lipid raft microdomain distribution, while the dimeric form is distributed in a non-raft microdomain (D'Ambrosi et al. 2007). Microdomains, such as a lipid raft, are known to be insoluble in Triton X-100 due to the fact that they are rich in cholesterol and sphingolipids. To examine the distribution of the dimeric P2Y6 receptor protein in raft or non-raft microdomains in WT- and SD-Mg, Triton X-100-treated cell lysates were fractionated by sucrose gradient centrifugation, followed by immunoblotting. We confirmed that the dimeric P2Y6 receptor protein was distributed in a non-raft microdomain in WT- and SD-Mg (Supplementary Fig. 3).

GD3 synthase and GM2/GD2 synthase double knockout mice have disordered lipid rafts, complement activation, and subsequent inflammation, suggesting that gangliosides are essential in the maintenance of lipid rafts (Ohmi et al. 2011). We next analyzed the amount of lipid rafts of both WT- and SD-Mg. There was little difference in the distribution of flotillin-1, a raft marker, between WT- and SD-Mg (Supplementary Fig. 3). However, cytochemical staining with an antibody against flotillin-1 indicated that the expression of flotillin-1 was decreased in SD-Mg compared with WT-Mg (Fig. 4a and Supplementary Fig. 4a). To confirm that the fluorescence signals represented the lipid raft microdomains, WT- and SD-Mg were treated with methyl- β -cyclodextrin (M β CD), which

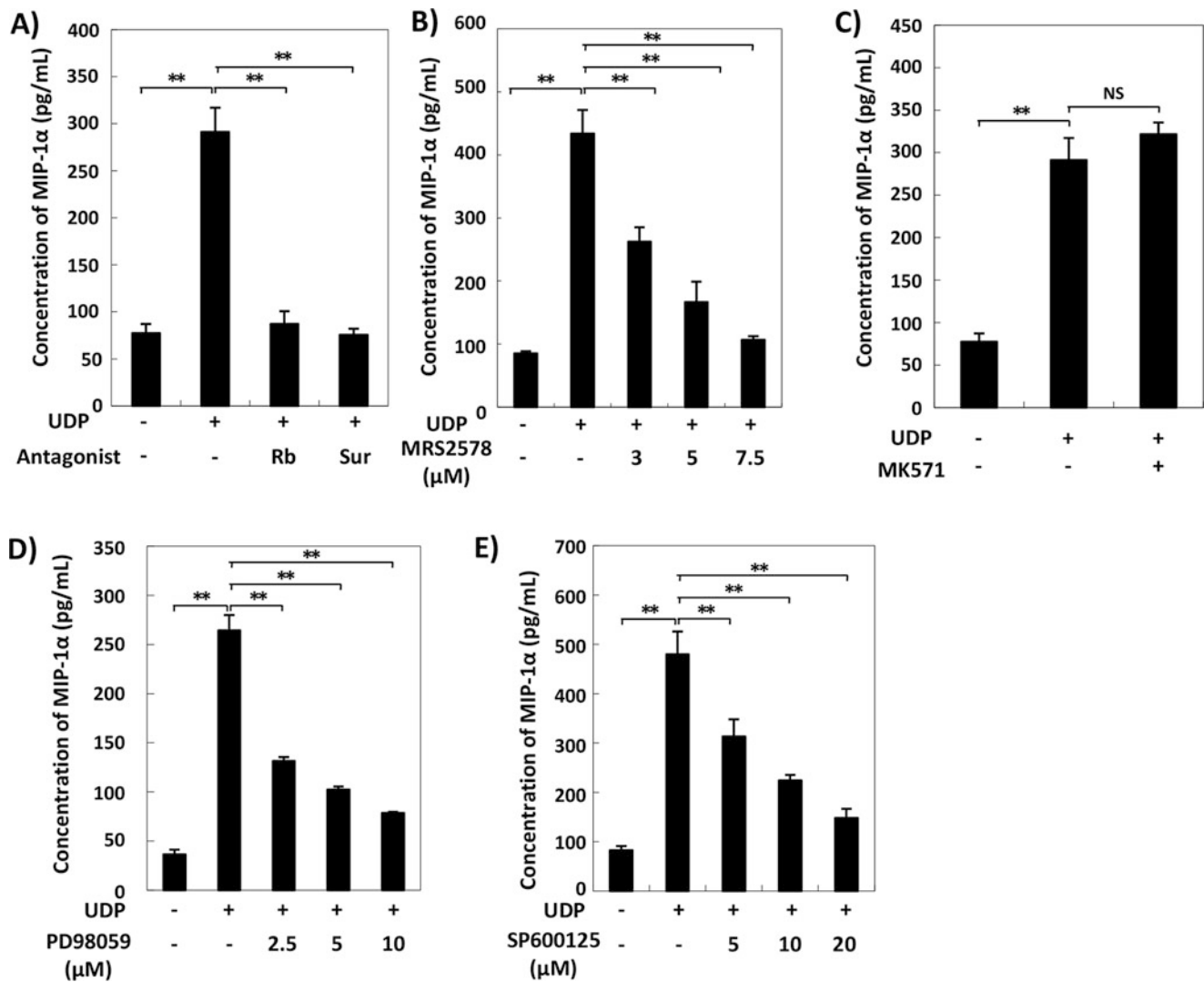


Fig. 2 Inhibition of UDP-induced MIP-1 α production in SD-Mg following treatment with a P2Y6 receptor antagonist, ERK inhibitor, or JNK inhibitor. (a–e) WT- and SD-Mg were pretreated with the indicated concentrations of antagonists or inhibitors for 30 min and then treated with UDP (0.25 μ M) for 6 h. The amounts of MIP-1 α in

the CM of the cells were measured using an ELISA kit ($n = 3$). For this inhibition assay, (a) Reactive Blue (Rb), suramin (Sur), (b) MRS2578, (c) MK571, (d) PD98059, and (e) SP600125 were used. Values represent the mean \pm S.E. Significance was evaluated using ANOVA with LSD post hoc test. ** $P < 0.01$

disrupts lipid rafts, followed by immunocytostaining. Disruption of the lipid rafts by treatment with M β CD reduced the intensity of flotillin-1 immunofluorescence, indicating that the fluorescence signals represented the lipid raft microdomains (Fig. 4a, Supplementary Fig. 4b, c). Thus, these data demonstrated that the maintenance of the lipid rafts was disordered in SD-Mg.

We next demonstrated that pretreatment with M β CD enhanced UDP-induced MIP-1 α production in both WT- and SD-Mg (Fig. 4b), suggesting that the disruption of lipid rafts enhanced the reaction to UDP in WT- and SD-Mg. We had expected that the disordered maintenance of lipid rafts

would enhance the dimeric formation of P2Y6 receptors in non-lipid rafts in SD-Mg, causing the enhanced response of SD-Mg to UDP under MIP-1 α upregulation; however, there was little difference in the amount of the dimeric P2Y6 receptor protein in non-lipid rafts in SD-Mg, with or without M β CD (data not shown).

A recent study reported that GM2 gangliosides are present in lipid rafts from the brain of a mouse model of Sanfilippo syndrome, a lysosomal disease (Dawson et al. 2012). We additionally determined whether accumulated GM2 gangliosides were distributed in the lipid rafts. Significant granular immunofluorescence for GM2 was

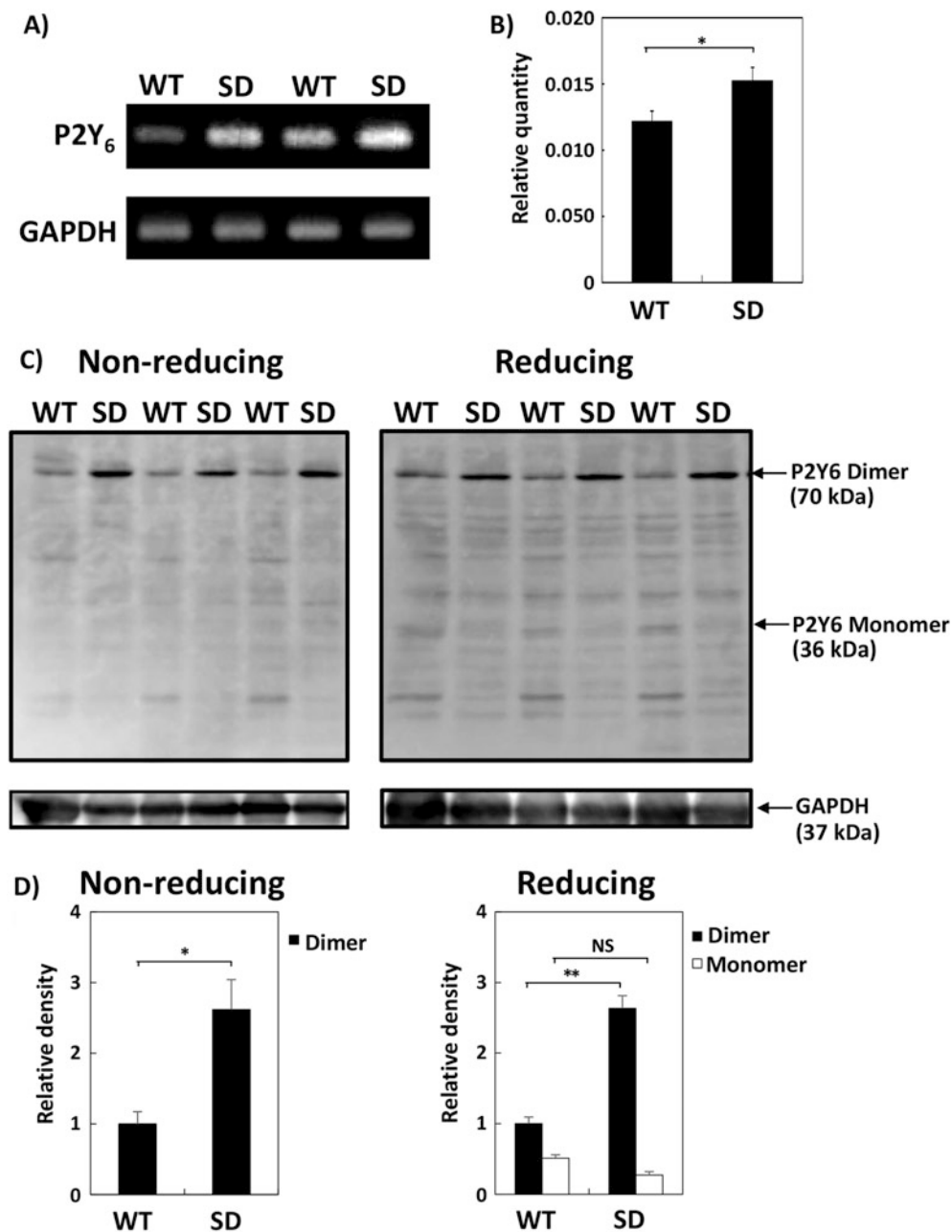


Fig. 3 Increase in the expression of P2Y₆ receptor in SD-Mg compared with WT-Mg. **(a)** An equal amount of PCR products was subjected to electrophoresis, stained with ethidium bromide, and then visualized under UV light. **(b)** mRNA expression levels of the P2Y₆ receptor relative to those of GAPDH were measured by a real-time PCR analysis ($n = 3$). **(c)** The cell lysates were subjected to immunoblotting using an antibody against the P2Y₆ receptor under

nonreducing or reducing conditions. **(d)** A densitometry analysis was performed using a RAS3000 image system. The bar graphs represent the relative density of P2Y₆ receptor protein normalized to that of GAPDH ($n = 3$). Values represent the mean \pm S.E. Significance was evaluated using Student's *t*-test or ANOVA with LSD post hoc test. * $P < 0.05$, ** $P < 0.01$

observed in SD-Mg, while the fluorescence in WT-Mg was below the detection limit. The merged image showed little overlapping of the GM2 signals with the lipid rafts (Supplementary Fig. 5), suggesting that GM2 gangliosides are most likely not component of the lipid rafts in SD-Mg.

Discussion

A recent study demonstrated the existence of uracil nucleotides, including UDP, in the brain extracellular fluid obtained from freely moving rats (Cansev et al. 2015). The excitotoxicity of brain injury induced by kainic acid

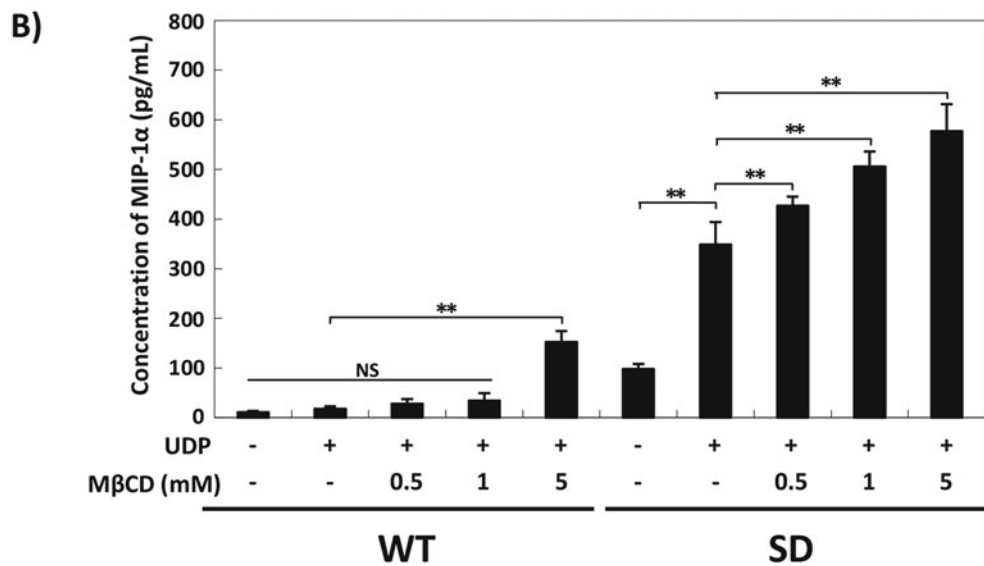
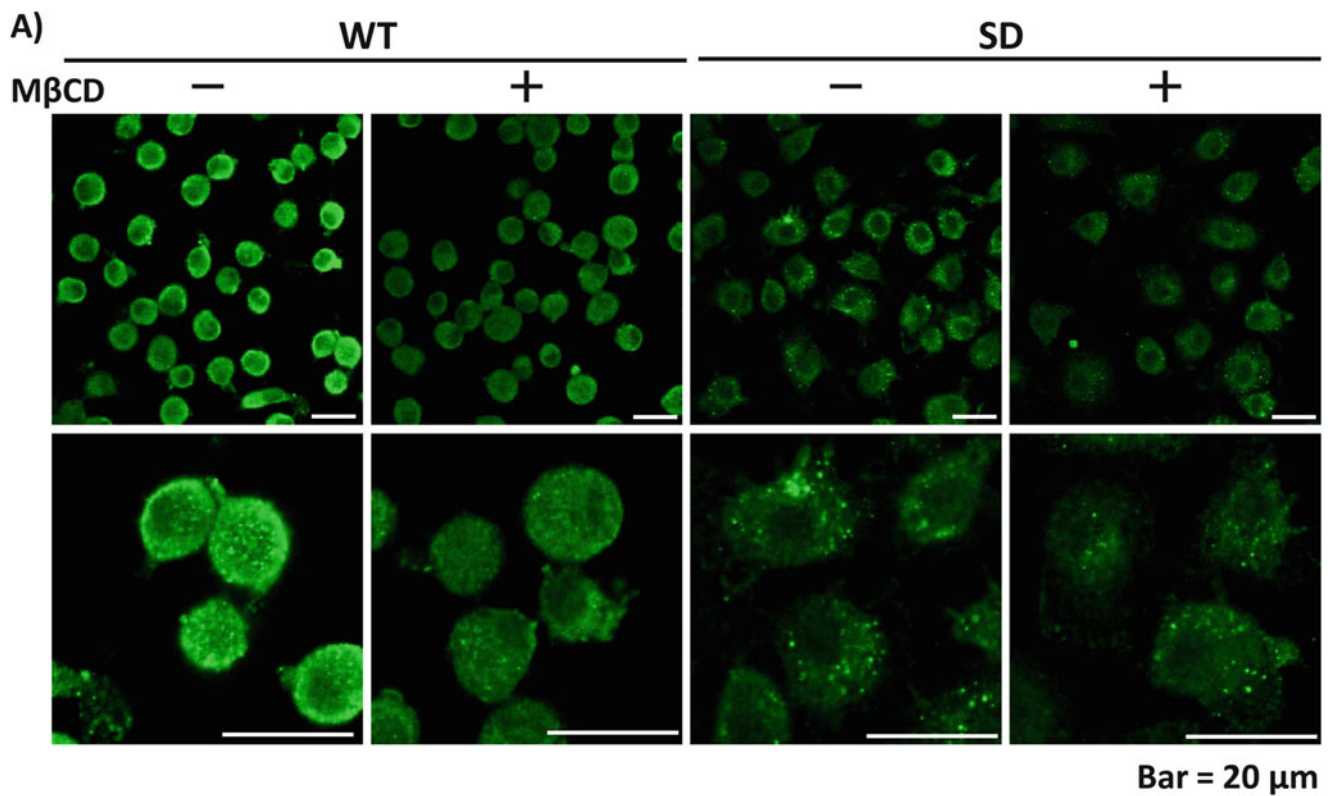


Fig. 4 Enhanced UDP-induced MIP-1α production by the disruption of lipid rafts in WT- and SD-Mg. **(a)** The neurons were immunostained with an antibody against flotillin-1 ($n = 3$). The representative images were acquired using a confocal laser microscope. Scale bar = 20 μm. **(b)** WT- and SD-Mg were pretreated with the indicated

concentrations of MβCD for 30 min and then treated with UDP (0.25 μM) for 6 h. The amounts of MIP-1α in the CM of the cells were measured using an ELISA kit ($n = 3$). Values represent the mean ± S.E. Significance was evaluated using ANOVA with LSD post hoc test. ****** $P < 0.01$

increases the level of extracellular UTP/UDP in the brain of rats. Microglia recognize this extracellular UDP leakage from injured or damaged neuronal cells, leading to the removal of the dying cells or their debris (Koizumi et al. 2007). These findings suggest that UDP is an important

neurotransmitter for microglia to regulate their functions physiologically and pathologically. Our present study demonstrated that UDP induces the production of MIP-1α in SD-Mg, but not WT-Mg, suggesting that UDP may cause the abnormal production of MIP-1α by microglia in the

brain of SD. The extracellular UDP-induced MIP-1 α might attract more microglia to the injured or damaged area, resulting in a rapid microglial inflammation in the progression of SD. Our supplemental experiment showed that the mRNA expression levels of IL-1 β and TNF- α increased in SD-Mg in comparison to WT-Mg (Supplementary Fig. 6), indicating that SD-Mg is more activated than WT-Mg due to the excessive accumulation of undegraded substrates. The different activation states of WT- and SD-Mg may lead to differences in the response to UDP.

We previously reported that the activation of PLC, PKC, ERK, and JNK mediates the enhanced production of MIP-1 α in SD-Mg (Kawashita et al. 2009). P2Y6 receptor couples to G_q protein to activate PLC β and mobilize intracellular Ca²⁺ (Erb and Weisman 2012) and also modulates several cellular functions through the activation of ERK, JNK, or PKC (Kim et al. 2003; Li et al. 2014). Our present study demonstrated that the activation of P2Y6 receptor, ERK, and JNK was involved in the UDP-induced MIP-1 α production in SD-Mg, thus suggesting that the activation of PLC, PKC, ERK, and JNK should be critical signal transduction molecules in the transmitter-induced abnormal production of MIP-1 α in an autocrine or paracrine manner in SD-Mg.

It has been previously reported that P2Y6 receptors form homodimers that are thought to be involved in receptor signaling, and the dimeric P2Y6 receptors exist in a non-raft microdomain (D'Ambrosi et al. 2007). In this study, the protein expression of the dimeric P2Y6 receptor, as well as the mRNA expression of P2Y6 receptor, was found to increase in SD-Mg in comparison to WT-Mg. We also observed the disordered maintenance of lipid rafts in SD-Mg in comparison to WT-Mg. In addition, the disruption of the lipid rafts enhanced UDP-induced MIP-1 α production in both WT- and SD-Mg, suggesting that lipid raft formation likely plays an important role in regulating UDP-P2Y6 receptor signaling. Contrary to our expectations, the disruption of lipid rafts did not result in an increase in the number of dimeric P2Y6 receptors in non-lipid rafts in SD-Mg, suggesting that the disordered maintenance of lipid rafts was most likely not involved in the enhanced dimeric formation in SD-Mg. Thus, these findings suggest that both the increase in the expression level of dimeric P2Y6 receptor and the disruption of lipid rafts may independently cause the enhanced response of SD-Mg to UDP in MIP-1 α production, compared with that of WT-Mg.

MIP-1 α is a crucial factor for microglia-mediated neuroinflammation in SD, and the downregulation of the abnormal production of MIP-1 α by microglia possibly delays the onset or progression of SD (Wu and Proia 2004; Tsuji et al. 2005). We previously reported that an agonist of

EP2 or EP4 receptor suppresses the abnormal production of MIP-1 α in SD-Mg (Kawashita et al. 2011). The findings of this study suggest that the P2Y6 receptor antagonist is therefore a novel potential therapeutic target for reducing the abnormal production of MIP-1 α in the brain of SD.

Acknowledgments Technical support for the experiments was provided by Dr. K. Nakayama from National Institute of Advanced Industrial Science and Technology.

Synopsis

UDP enhances MIP-1 α production through the increased expression of the dimeric P2Y6 receptors and the disordered maintenance of the lipid rafts in microglia derived from Sandhoff disease model mice.

Compliance with Ethics Guidelines

Conflict of Interest

Eri Kawashita, Daisuke Tsuji, Yosuke Kanno, Kaho Tsuchida, and Kohji Itoh declare that they have no conflict of interest.

Animal Rights

All institutional and national guidelines for the care and use of laboratory animals were followed.

Details of the Contributions of Individual Authors

EK and KI planned the experiments. EK and DT conducted the experiments. EK, DT, and KT analyzed the data. EK, DT, YK, KT, and KI interpreted the data. EK wrote the paper.

References

- Bradbury AM, Cochran JN, McCurdy VJ et al (2013) Therapeutic response in feline Sandhoff disease despite immunity to intracranial gene therapy. *Mol Ther* 21:1306–1315
- Cansev M, Orhan F, Yaylagul EO et al (2015) Evidence for the existence of pyrimidinergic transmission in rat brain. *Neuropharmacology* 91:77–86
- D'Ambrosi N, Iafrate M, Saba E, Rosa P, Volonte C (2007) Comparative analysis of P2Y4 and P2Y6 receptor architecture in native and transfected neuronal systems. *Biochim Biophys Acta* 1768:1592–1599
- Davalos D, Grutzendler J, Yang G et al (2005) ATP mediates rapid microglial response to local brain injury in vivo. *Nat Neurosci* 8:752–758

- Dawson G, Fuller M, Helmsley KM et al (2012) Abnormal gangliosides are localized in lipid rafts in Sanfilippo (MPS3a) mouse brain. *Neurochem Res* 37:1372–1380
- Erb L, Weisman GA (2012) Coupling of P2Y receptors to G proteins and other signaling pathways. *Wiley Interdiscip Rev Membr Transp Signal* 1:789–803
- Ikeda M, Tsuno S, Sugiyama T et al (2013) Ca²⁺ spiking activity caused by the activation of store-operated Ca²⁺ channels mediates TNF- α release from microglial cells under chronic purinergic stimulation. *Biochim Biophys Acta* 1833:2573–2585
- Jeyakumar M, Thomas R, Elliot-Smith E et al (2003) Central nervous system inflammation is a hallmark of pathogenesis in mouse models of GM1 and GM2 gangliosidosis. *Brain* 126:974–987
- Kawashita E, Tsuji D, Kawashima N, Nakayama K, Matsuno H, Itoh K (2009) Abnormal production of macrophage inflammatory protein-1 α by microglial cell lines derived from neonatal brains of Sandhoff disease model mice. *J Neurochem* 109:1215–1224
- Kawashita E, Tsuji D, Toyoshima M, Kanno Y, Matsuno H, Itoh K (2011) Prostaglandin E2 reverses aberrant production of an inflammatory chemokine by microglia from Sandhoff disease model mice through the cAMP-PKA pathway. *PLoS One* 6:e16269
- Kim SG, Gao ZG, Soltysiak KA, Chang TS, Brodie C, Jacobson KA (2003) P2Y6 nucleotide receptor activates PKC to protect 1321N1 astrocytoma cells against tumor necrosis factor-induced apoptosis. *Cell Mol Neurobiol* 23:401–418
- Kim B, Jeong HK, Kim JH, Lee SY, Jou I, Joe EH (2011) Uridine 5'-diphosphate induces chemokine expression in microglia and astrocytes through activation of the P2Y6 receptor. *J Immunol* 186:3701–3709
- Koizumi S, Shigemoto-Mogami Y, Nasu-Tada K et al (2007) UDP acting at P2Y6 receptors is a mediator of microglial phagocytosis. *Nature* 446:1091–1095
- Kotani M, Ozawa H, Kawashima I, Ando S, Tai T (1992) Generation of one set of monoclonal antibodies specific for a-pathway ganglio-series gangliosides. *Biochim Biophys Acta* 1117:97–103
- Lee JP, Jeyakumar M, Gonzalez R et al (2007) Stem cells act through multiple mechanisms to benefit mice with neurodegenerative metabolic disease. *Nat Med* 13:439–447
- Li R, Tan B, Yan Y et al (2014) Extracellular UDP and P2Y6 function as a danger signal to protect mice from vesicular stomatitis virus infection through an increase in IFN- β production. *J Immunol* 193:4515–4526
- Mahuran DJ (1999) Biochemical consequences of mutations causing the GM2 gangliosidosis. *Biochim Biophys Acta* 1455:105–138
- Matsuoka K, Tsuji D, Aikawa S, Matsuzawa F, Sakuraba H, Itoh K (2010) Introduction of an N-glycan sequon into HEXA enhances human beta-hexosaminidase cellular uptake in a model of Sandhoff disease. *Mol Ther* 18:1519–1526
- Mellor EA, Maekawa A, Austen KF, Boyce JA (2001) Cysteinyl leukotriene receptor 1 is also a pyrimidinergic receptor and is expressed by human mast cells. *Proc Natl Acad Sci U S A* 98:7964–7969
- Mellor EA, Frank N, Soler D et al (2003) Expression of the type 2 receptor for cysteinyl leukotrienes (CysLT2R) by human mast cells: functional distinction from CysLT1R. *Proc Natl Acad Sci U S A* 100:11589–11593
- Nimmerjahn A, Kirchhoff F, Helmchen F (2005) Resting microglial cells are highly dynamic surveillants of brain parenchyma in vivo. *Science* 308:1314–1318
- Norflus F, Tiffit CJ, McDonald MP et al (1998) Bone marrow transplantation prolongs life span and ameliorates neurologic manifestations in Sandhoff disease mice. *J Clin Invest* 101:1881–1888
- Ohmi Y, Tajima O, Ohkawa Y et al (2011) Gangliosides are essential in the protection of inflammation and neurodegeneration via maintenance of lipid rafts: elucidation by a series of ganglioside-deficient mutant mice. *J Neurochem* 116:926–935
- Sango K, Yamanaka S, Hoffmann A et al (1995) Mouse models of Tay-Sachs and Sandhoff diseases differ in neurologic phenotype and ganglioside metabolism. *Nat Genet* 11:170–176
- Tsuji D, Kuroki A, Ishibashi Y et al (2005) Specific induction of macrophage inflammatory protein 1- α in glial cells of Sandhoff disease model mice associated with accumulation of N-acetylhexosaminyl glycoconjugates. *J Neurochem* 92:1497–1507
- Uesugi A, Kataoka A, Tozaki-Saitoh H et al (2012) Involvement of protein kinase D in uridine diphosphate-induced microglial macropinocytosis and phagocytosis. *Glia* 60:1094–1105
- von Kugelgen I (2006) Pharmacological profiles of cloned mammalian P2Y-receptor subtypes. *Pharmacol Ther* 110:415–432
- Wada R, Tiffit CJ, Proia RL (2000) Microglial activation precedes acute neurodegeneration in Sandhoff disease and is suppressed by bone marrow transplantation. *Proc Natl Acad Sci U S A* 97:10954–10959
- Wortmann SB, Lefebvre DJ, Dekomien G, Willemsen MA, Wevers RA, Morava E (2009) Substrate deprivation therapy in juvenile Sandhoff disease. *J Inher Metab Dis* 32(Suppl 1):S307–S311
- Wu YP, Proia RL (2004) Deletion of macrophage-inflammatory protein 1 α retards neurodegeneration in Sandhoff disease mice. *Proc Natl Acad Sci U S A* 101:8425–8430